Impact of declining Arctic sea ice on winter snowfall

Jiping Liu[a,b,1], Judith A. Curry[a], Huijun Wang[b], Mirong Song[b], and Radley M. Horton[c]

[a]School of Earth and Atmospheric Sciences, Georgia Institute of Technology, Atlanta, GA 30332; [b]LASG, Institute of Atmospheric Physics, Chinese Academy of Sciences, Beijing, 100029, China; and [c]Columbia University Center for Climate Systems Research, New York, NY, 10025

Edited by Mark H. Thiemens, University of California San Diego, La Jolla, CA, and approved January 17, 2012 (received for review September 9, 2011)

While the Arctic region has been warming strongly in recent decades, anomalously large snowfall in recent winters has affected large parts of North America, Europe, and east Asia. Here we demonstrate that the decrease in autumn Arctic sea ice area is linked to changes in the winter Northern Hemisphere atmospheric circulation that have some resemblance to the negative phase of the winter Arctic oscillation. However, the atmospheric circulation change linked to the reduction of sea ice shows much broader meridional meanders in midlatitudes and clearly different interannual variability than the classical Arctic oscillation. This circulation change results in more frequent episodes of blocking patterns that lead to increased cold surges over large parts of northern continents. Moreover, the increase in atmospheric water vapor content in the Arctic region during late autumn and winter driven locally by the reduction of sea ice provides enhanced moisture sources, supporting increased heavy snowfall in Europe during early winter and the northeastern and midwestern United States during winter. We conclude that the recent decline of Arctic sea ice has played a critical role in recent cold and snowy winters.

During the past few winters, North America, Europe, and east Asia have experienced anomalously cold conditions, along with record snowfalls (1–3). Anomalously heavy snowfall wrought havoc in large parts of the United States and northwestern Europe for the winters of 2009–2010 and 2010–2011. A series of snowstorms hit central and southern China for the winter of 2007–2008. Persistent snow, freezing rain, and cold temperature resulted in disruptions in transport, energy supply, and power transmission and damage to agriculture (1–3). The causes of the recent severe winters are unclear, particularly in context of the amplified warming in the Arctic (4, 5) that has contributed to the reduction of sea ice.

Some explanations have been offered for the recent severe winters from the perspective of dominant modes of climate variability. Seager et al. (6) suggest that the anomalously high levels of snowfall in the mid-Atlantic states of the United States and northwestern Europe for the winter of 2009–2010 were forced by the negative phase of the North Atlantic oscillation (NAO) and to a lesser extent by El Niño. Ratnam et al. (7) show that the heating associated with El Niño Modoki during boreal winter 2009–2010 accounts for most of the anomalous conditions observed over parts of North America and Europe. Cohen et al. (8) argue that the strong negative Arctic oscillation (AO) (9) for the winter of 2009–2010 is the major contributing factor to severe winter weather in the Northern Hemisphere. As shown in Fig. S1, significantly above-normal winter snow cover has been present in large parts of the northern United States, northwestern and central Europe, and northern and central China for the four winters since the record low Arctic sea ice during 2007. However, no clear persistent out-of-phase NAO/AO-snow cover and in-phase El Niño-snow cover relationship are evident in the observations for the past four winters (Fig. S2). Diminishing Arctic sea ice and its potential climatic impacts have received increasing attention (10–12); i.e., many studies have demonstrated that regional loss of Arctic sea ice can have hemispheric consequences in atmospheric circulation (13–19). Recent studies show that cold conditions and increased snow cover over Siberia in autumn are correlated with reduced September sea ice cover in the Pacific sector of the Arctic (20, 21). Furthermore, Fig. S2 does support a persistent out-of-phase sea ice-snow cover relationship for the past four winters.

Here we extend previous studies by combining observational data analyses and numerical experiments, demonstrating how anomalously large snowfall in large parts of the Northern Hemisphere continents in recent winters are linked to diminishing Arctic sea ice.

Results

For the period of the available satellite data record (since the late 1970s), Arctic sea ice extent has been decreasing in all months, with the most pronounced loss in September (22). As shown in Fig. 1, the autumn (September, October, November) Arctic sea ice area has declined 27.3% for 1979–2010 (relative to the 1979–2000 average, >99% significance). In 2007, the autumn Arctic sea ice area reached an unexpectedly low value, outpacing that simulated by IPCC AR4 climate models in response to greenhouse warming (23). Our speculation surrounding the connection between the accelerated decline of Arctic sea ice for the past few years and recent anomalously cold and snowy winters over northern continents is based on the following mechanisms. When highly reflective sea ice is replaced by open water during the ice melting period, there is a substantial solar heat input directly into the ocean, increasing the heat stored in the upper ocean. For example, the cumulative solar heat input in the Beaufort Sea during the ice melting period in 2007 can be a factor of two to five higher than climatology, which is sufficient to warm the upper 5 m of the ocean by 5 °C (24). The loss of sea ice in the Canada basin has also been accompanied by the widespread appearance of a near-surface temperature maximum at 25- to 35-m depth due to penetrating solar radiation (25). Warming of the upper ocean retards the recovery of sea ice during the fall freeze-up. As a result, the ice coverage in late autumn and early winter for the past few years is significantly below the mean of 1979–2000, exceeding two standard deviation of ice variability (Fig. S3). The anomalously warm, ice-free ocean water increases the ocean surface flux of heat and moisture into the atmosphere in late autumn and early winter, which in turn has substantial impacts on winter atmospheric circulation.

By examining observational data for the period 1979–2010, the fraction of winter (December, January, February) climate of the extratropical Northern Hemisphere that is linearly congruent with the interannual variability of autumn Arctic sea ice is found by regressing winter anomalies of snow cover and atmospheric fields from the National Center for Environmental Prediction reanalysis II (NCEP2) onto the detrended autumn Arctic sea ice area. The regression map between sea ice area and snow cover reveals that snow cover anomalies over the Northern Hemisphere continents are closely linked to Arctic sea ice variability. A de-

Author contributions: J.L., J.A.C., and H.W. designed research; J.L. and M.S. performed research; J.L. and M.S. analyzed data; and J.L., J.A.C., and R.M.H. wrote the paper.

The authors declare no conflict of interest.

This article is a PNAS Direct Submission.

[1]To whom correspondence should be addressed. E-mail: jliu@eas.gatech.edu.

This article contains supporting information online at www.pnas.org/lookup/suppl/doi:10.1073/pnas.1114910109/-/DCSupplemental.

crease of autumn Arctic sea ice of 1 million km^2 corresponds to a significantly above-normal winter snow cover (>3-12%) in large parts of the northern United States, northwestern and central Europe, and northern and central China (Fig. 1*B*).

One important contributor to the anomalously large snowfall in recent winters is changes in atmospheric circulation linked to diminishing Arctic sea ice. The regression map between sea ice area and sea level pressure (SLP) reveals that following anomalously low ice coverage in autumn, the winter SLP is substantially higher over the Arctic Ocean, the northern Atlantic, and much of high-latitude continents, which is compensated by lower SLP in midlatitudes (Fig. 2*A*). This pattern shows some resemblance to the negative phase of the winter AO (Fig. 2*B*). However, some significant differences are noticed. First, the pattern linked to the reduction of autumn sea ice shows broader meridional meanders in midlatitudes rather than the zonal symmetry associated with the winter AO pattern (Fig. 2 *A* vs. *B*). A recent study also noted that recent loss of summer sea ice in the Arctic is directly connected to a shift to a more meridional atmospheric circulation pattern in the following autumn and suggested that increased modification of atmospheric circulation pattern would be anticipated with continuing loss of summer sea ice to less than 20% of its climatology over the next decades (26). Second, the pattern linked to the reduction of autumn sea ice shows clearly different interannual variability relative to the classical winter AO pattern;

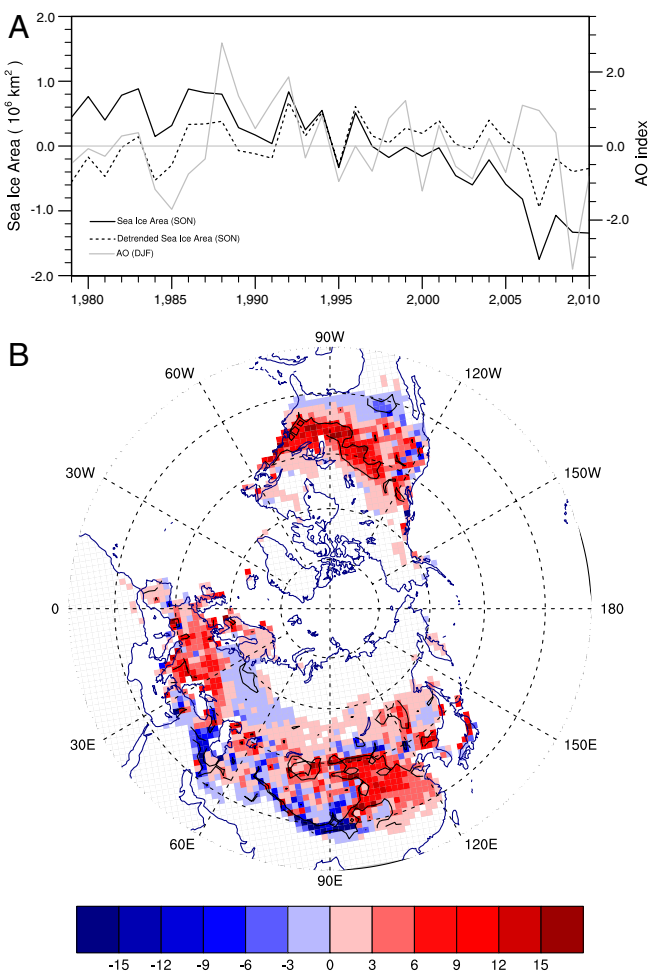

Fig. 1. (*A*) Time series of actual and detrended autumn Arctic sea ice area anomaly (×10^6 km^2) and winter AO index and (*B*) linear regression of winter snow cover anomalies (%) on the detrended autumn Arctic sea ice area anomaly (regions within contours denote the regression above 95% confidence level).

i.e., the detrended autumn Arctic sea ice and winter AO indices have weak correlation (0.28), only accounting for approximately 8% of the shared variance. Thus, the atmospheric circulation change linked to the reduction of sea ice is different from the classical AO.

Under such circulation change, the prevailing westerly winds blowing across the North Atlantic (North Pacific) from Canada (offshore of Japan) to Europe (Canada) are weakened. As shown in the vertical cross-section of the regression of the winter zonal mean zonal wind anomalies on the detrended autumn Arctic sea ice area anomaly (Fig. S4), the zonal wind anomalies are negative in midlatitudes extending from the surface to the troposphere, which represent 20–60% of the magnitude of the climatological zonal wind. This suggests a shift to a more meridional anomalous wind pattern in winter congruent with the reduction of the autumn Arctic sea ice. Weak westerly winds tend to enhance broader meanders that are likely to form blocking circulations. Fig. 3*A* shows that associated with the reduction of autumn sea ice, there is an increased incidence of blockings during winter over much of northern high-latitude continents, with the most pronounced increase in eastern Europe, central Siberia, southern Alaska, and the northwestern United States (20–60% greater than climatology). These blocking patterns favor more frequent incursions of cold air masses from the Arctic into mid- and low-latitude of northern continents. As shown in Fig. 3*B*, there is an increased frequency of cold events over much of northern continents, with the most pronounced increase in the eastern and midwestern United States, northwestern Europe, between mid-east and central Asia, and central and south China (20–60% greater than climatology). This leads to cold conditions over much of northern continents; i.e., temperature anomalies extending southeastward from northwestern Canada to the southeastern United States, and eastward/southeastward from northwestern Europe to central China can be 2–3 °C below-normal in association with 1 million km^2 decrease of the autumn Arctic sea ice (Fig. 2*C*).

The only notable exception is northeastern Canada and Greenland, where weak westerly winds favors more frequent incursions of warm air masses from the North Atlantic. This leads to warm anomalies there (Fig. 2*C*), helping to explain extremely low ice coverage observed in Baffin/Hudson Bay, Davis Strait, the Labrador Sea, and Gulf of Saint Lawrence in recent winters, particularly in 2009–2010 and 2010–2011 (Fig. S5).

Another potential contributor to anomalously large snowfall in recent winters is changes in atmospheric water vapor content over northern high latitudes. The rapid retreat of sea ice in summer and slow recovery of sea ice in autumn, particularly after 2007, greatly enhances moisture flux from the ocean to the atmosphere. This increases the humidity of Arctic air masses remarkably during ice growth period. Following anomalously low ice coverage in autumn, the regions with the most pronounced increase of specific humidity (integrated from surface to 700 hPa) during late autumn and early winter are found in northern/eastern Europe, far eastern Siberia, and western Alaska (Fig. 3*C*). During winter, the regions showing the most pronounced increase of specific humidity mainly shift to northeastern North America due to the aforementioned anomalously low winter ice coverage in Baffin/Hudson Bay, Davis Strait, the Labrador Sea, and Gulf of Saint Lawrence (Fig. 3*D*). The increase of humidity in autumn provides an additional local moisture source to Europe, in addition to circulation change induced moisture transport from midlatitudes through shifting the storm track southward and increasing storminess over the Mediterranean (Fig. 2*A*). Meanwhile, cold air masses that develop over central Siberia more readily spill over into Europe. Thus, in Europe, it is more likely to see anomalous snowstorm events during late autumn and early winter, which was the case for recent winters. Similarly, the increase of humidity in winter provides an extra local moisture source to northeastern North America. Together with enhanced cold air outbreaks in

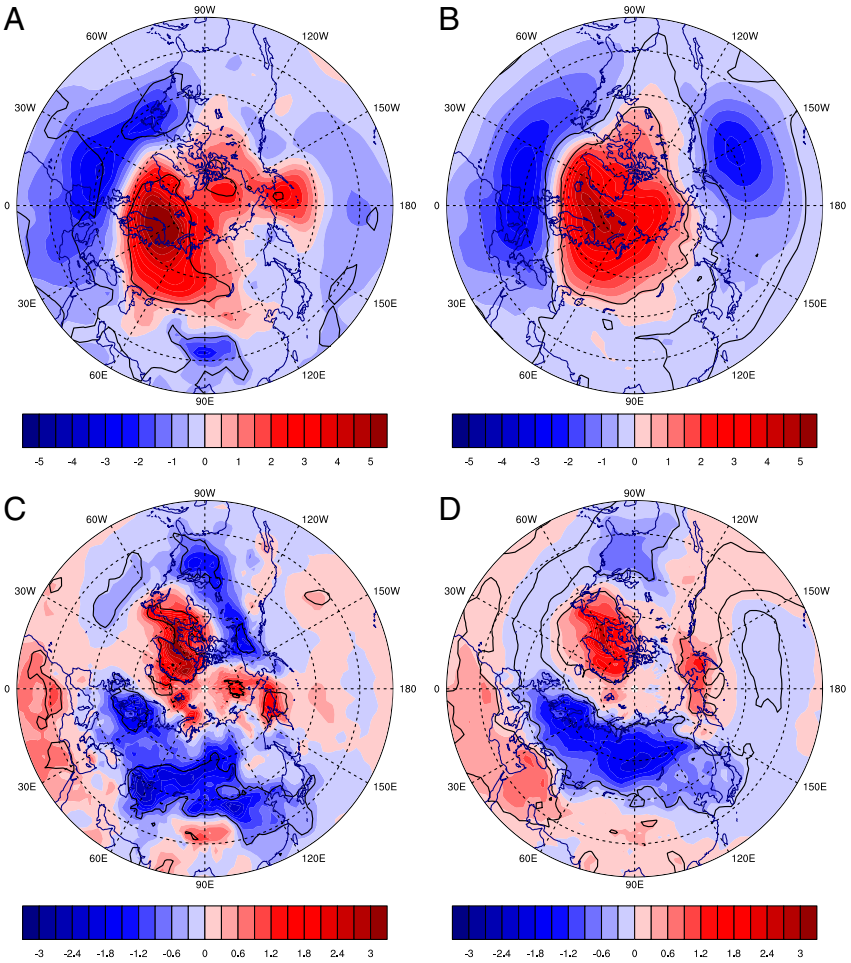

Fig. 2. Linear regression of winter sea level pressure (hPa, *Upper*) and surface air temperature (°C, *Lower*) on (*A* and *C*) the detrended autumn Arctic sea ice area anomaly (regions within contours denote the regression above 95% confidence level) and (*B* and *D*) AO index.

the eastern and midwestern United States, this increases the likelihood of anomalously snowstorm events in the northeastern and midwestern United States in winter and even persisting into early spring.

The ERA-interim reanalysis also suggests that the largest specific humidity increase during 1989–2008 is in the Arctic region, and a large portion of this enhanced moisture flux is due to diminishing Arctic sea ice through surface latent heat flux (27). Moreover, a recent study examined the predominant origin of water vapor in northern high latitudes during the ice growth period using water isotopes (deuterated water, HDO, and heavy oxygen water, $H_2^{18}O$) as tracers; i.e., isotopic values of water vapor originating from the Arctic Ocean have higher d-excess values than those of water vapor originating from lower latitudes, where d-excess value is defined as HDO minus $H_2^{18}O$. The high d-excess values of Arctic-origin air masses were observed in midautumn and gradually decreased to the global average in early winter (28). This further indicates that the moisture source in Europe (northeastern North America) might be primarily locally driven in late autumn and early winter (winter) and switches from locally driven to moisture transport from lower latitudes in early winter (late winter). Note that specific humidity decreases associated with the reduction of sea ice in the west north central United States and eastern China, although above-normal snow cover is observed there linked to the reduction of sea ice. This suggests that the moisture source for these regions might primarily come from lower latitudes.

To confirm the robustness of the changes of atmospheric circulation and water vapor content linked to the reduction of sea ice identified using the NCEP2 (atmospheric model only reanalysis), we repeat the above analyses using a new reanalysis, the NCEP Climate Forecast System Reanalysis (CFSR, executed in a coupled atmosphere-ocean-sea ice system). As shown in Fig. S6, the regression patterns of SLP, SAT, and specific humidity of the CFSR closely resemble to those of NCEP2.

To further interpret the observational data analyses, we conduct simulations with the National Center for Atmospheric Research Community Atmospheric Model Version 3.1 (29), for which sea surface temperatures (SST) and sea ice concentrations are specified as boundary conditions based on a merged product of the Hadley Centre sea ice and SST dataset and the National Oceanic and Atmospheric Administration weekly optimum interpolation SST analysis (30). The simulation configuration has a horizontal resolution of approximately 2.8° and 26 vertical levels extending up to 3.5 hPa. The impact of the diminishing Arctic sea ice during the freeze-up on atmospheric circulation is assessed by comparing two experiments with different seasonally varying sea ice distributions, with all other external variables held fixed. The control experiment is run with seasonally varying Arctic sea ice based on the climatology of the Hadley Centre sea ice concentrations for 1979–2010. The perturbed experiment is integrated with prescribed sea ice loss in autumn and winter based on regressions of the satellite-derived autumn and winter Arctic sea ice concentrations obtained from the National Snow and Ice Data Center, respectively, on the standardized autumn Arctic sea ice index for

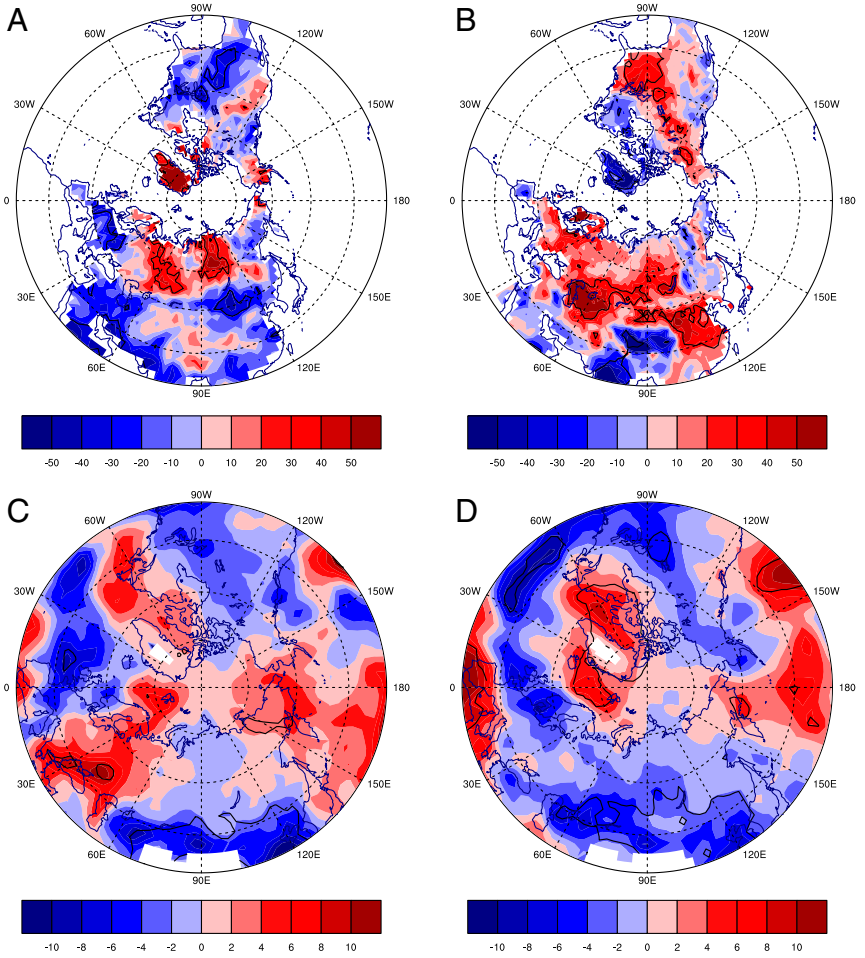

Fig. 3. (*A*) Ratio (%) between linear regression of incidence of winter blockings on the detrended autumn Arctic sea ice area anomaly and winter blocking climatology during 1979–2010. *B* is similar to *A* except for winter cold events, and linear regression of specific humidity (integrated from surface to 700 hPa, kg/kg) in (*C*) November-December (late autumn to early winter) and (*D*) December-January (winter) on the detrended autumn Arctic sea ice area anomaly (regions within contours denote the regression above 95% confidence level).

1979–2010 that are statistically significant at the 90% confidence level (Fig. 4 *A* and *B*). Thus, the prescribed winter sea ice anomalies can be considered as the autumn sea ice anomalies persisting into winter. Global SSTs in both experiments are set to their climatological monthly values based on the merged SST dataset for the same period of record used for the sea ice climatology in the control experiment. In addition, in the perturbed experiment, in those areas where sea ice is removed, SST is set to freezing point of seawater, $-1.8°C$. To help gauge confidence in the model response's to sea ice losses, each experiment consists of 20 ensemble members with slightly different initial conditions. The response of the model to the prescribed sea ice losses is examined by differencing SLP and SAT between the ensemble mean of the perturbed and control experiments.

As shown in Fig. 4 *C* and *D*, the diminishing Arctic sea ice does induce positive SLP anomalies over high latitudes and negative SLP anomalies over midlatitudes in winter, which is accompanied by a significant surface warming in the Arctic Ocean and Greenland/northeastern Canada and cooling over northern North America, Europe, Siberia, and eastern Asia. Moreover, in late autumn and early winter, the regions showing the largest increase of specific humidity are found in Europe (Fig. 4*E*), whereas during winter the largest increase of specific humidity is mainly located in northeastern North America (Fig. 4*F*). While the regional details differ somewhat between the response of the modeled snowfall (Fig. S7) and the observation (Fig. 1*B*), the model simulation does show above-normal winter snowfall in large parts of the northern United States, central Europe, and northern and central China. The encouraging consistency between model simulations and observations support the hypothesis outlined above.

Discussion

The results of this study add to an increasing body of both observational and modeling evidence that indicates diminishing Arctic sea ice plays a critical role in driving recent cold and snowy winters over large parts of North America, Europe, and east Asia. The relationships documented here illustrate that the rapid loss of sea ice in summer and delayed recovery of sea ice in autumn modulates not only winter mean statistics (i.e., snow cover and temperature) but also the frequency of occurrence of weather events (i.e., cold air outbreaks). While natural chaotic variability remains a component of midlatitude atmospheric variability, recent loss of Arctic sea ice, with its signature on midlatitude atmospheric circulation, may load the dice in favor of snowier conditions in large parts of northern midlatitudes. The relationships elucidated here can be also of practical use in seasonal forecasting of snow and temperature anomalies over northern continents and assessing the potential risk of such events. If the decline of Arctic sea ice continues as anticipated by climate modeling results (31, 32), we speculate that episodes of the aforementioned circulation change will become more frequent, along with more persistent snowstorms over northern continents during winter. Year-to-year variations in autumnal sea ice area may provide a useful predictor of wintertime snowfall in these regions. Better

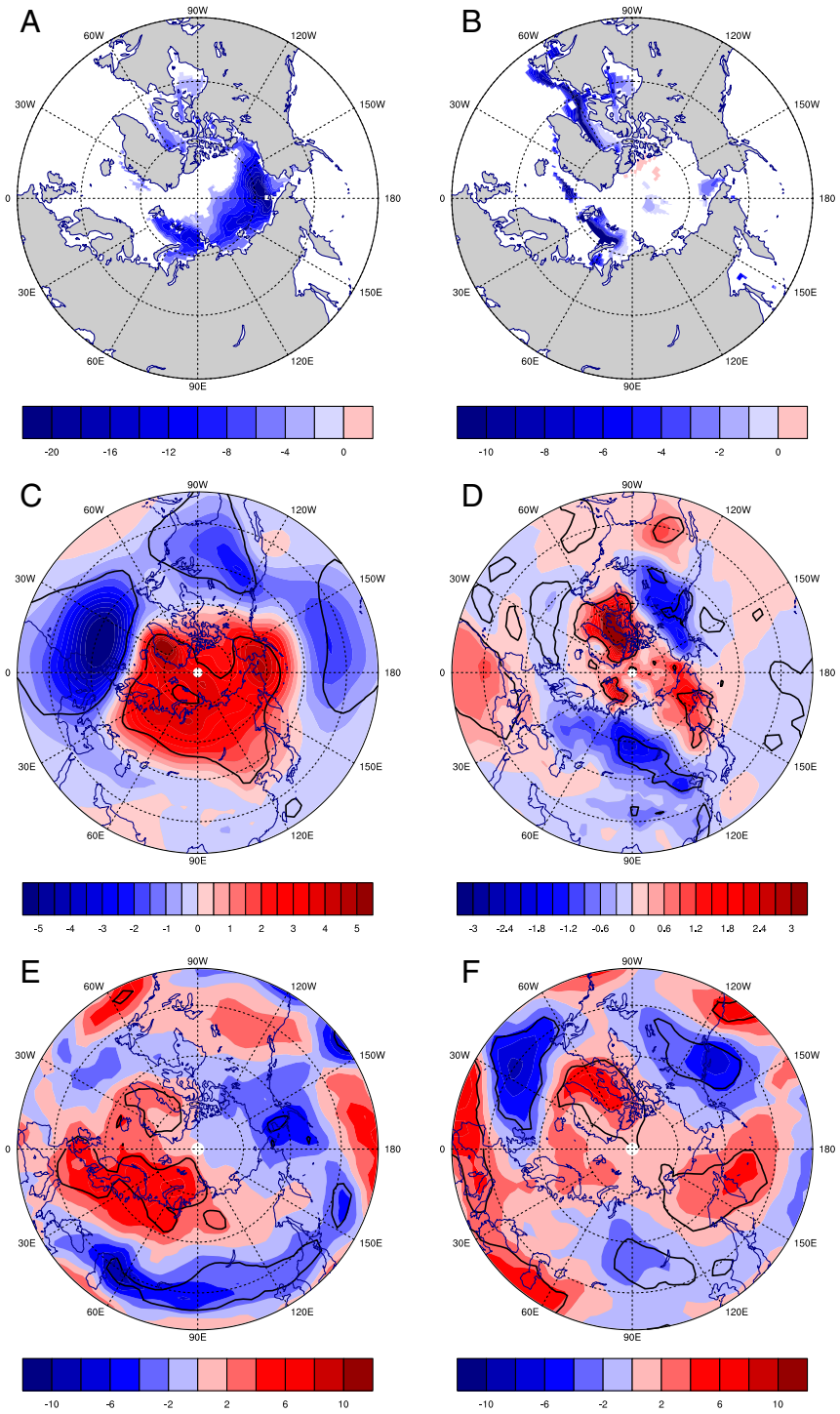

Fig. 4. Prescribed sea ice loss (%) in (*A*) autumn and (*B*) winter applied to the perturbed experiment and differences in (*C*) sea level pressure (hPa) and (*D*) surface air temperature (°C) in winter and specific humidity (integrated from surface to 700 hPa, kg/kg) in (*E*) November-December (late autumn to early winter) and (*F*) December-January (winter) between the perturbed and control experiments (regions within contours denote the model responses that are above 95% confidence level).

understanding of interactions between the diminishing Arctic sea ice and dominant modes of climate variability (i.e., NAO/AO, El Niño) and natural chaotic variability of the general circulation is a fertile area for further research, given the potential to improve seasonal forecasts.

Methods

The Arctic sea ice, obtained from the National Snow and Ice Data Center, is retrieved from the Scanning Multichannel Microwave Radiometer and the Special Sensor Microwave/Imager using a team algorithm (33). The snow cover is obtained from the Rutgers University Global Snow Lab, which has developed a satellite snow extent climate record back to late 1966 (http://climate.rutgers.edu/snowcover). The sea level pressure, surface air temperature, 500-hPa geopotential height, and specific humidity (from surface to 700 hPa) are obtained from the National Center for Environmental Prediction reanalysis II (NCEP2) (34) and the NCEP Climate Forecast System Reanalysis (CFSR, 35). Preliminary analysis indicates the CFSR is far superior in most respects to the reanalysis of the mid-1990s in both scope and quality, because it is executed

in a coupled mode with a more modern data assimilation system and forecast model (35).

Blocking involves the formation of quasi-stationary, long-lived (>7 days), closed anticyclonic circulation that temporarily divert the prevailing westerly flow of air in troposphere. Here blocking events are defined as intervals in which daily 500-hPa height from the NCEP2 reanalysis exceeds 1 standard deviation about its mean for five consecutive days (36). Cold air outbreaks often occur downstream of high-latitude blocking anticyclones. Here the cold events are defined as daily minimum temperature from the NCEP2 reanalysis 1.5 standard deviation below the climatological mean (36).

We regress winter mean anomaly fields upon the detrended autumn Arctic sea ice area anomaly time series and display the resulting regression coefficients. The amplitudes shown in the regression maps therefore correspond to anomaly values in that field that occur in association with 1 million km^2 anomaly in the autumn Arctic sea ice area and can thus be considered typical amplitudes.

ACKNOWLEDGMENTS. This research is supported by the National Aeronautics and Space Administration Energy and Water Cycle Study, National Science Foundation Polar Programs (0838920), 973 program (2011CB309704, 2009CB421406), and the National Natural Science Foundation of China (41176169).

1. World Meteorological Organization (2009) *WMO Statement on the Status of the Global Climate in 2008* (World Meteorological Organization, Geneva) WMO-No. 1039.
2. World Meteorological Organization (2010) *WMO Statement on the Status of the Global Climate in 2009* (World Meteorological Organization, Geneva) WMO-No. 1055.
3. World Meteorological Organization (2011) *WMO Statement on the Status of the Global Climate in 2010* (World Meteorological Organization, Geneva) WMO-No. 1074.
4. Solomon S, et al. (2007) *Climate Change 2007: The Physical Science Basis* (Cambridge Univ Press, Cambridge, UK).
5. Symon C, Arris L, Heal B (2004) *Arctic Climate Impact Assessment* (Cambridge Univ Press, Cambridge, UK).
6. Seager R, Kushnir Y, Nakamura J, Ting M, Naik N (2010) Northern Hemisphere winter snow anomalies: ENSO, NAO and the winter of 2009/10. *Geophys Res Lett*, 10.1029/2010GL043830.
7. Ratnam J, Behera S, Masumoto Y, Takahashi K, Yamagata T (2011) Anomalous climatic conditions associated with the El Niño Modoki during boreal winter of 2009. *Clim Dynam*, 10.1007/s00382-011-1108-z.
8. Cohen J, Foster J, Barlow M, Saito K, Jones J (2010) Winter 2009–2010: A case study of an extreme Arctic Oscillation event. *Geophys Res Lett*, 10.1029/2010GL044256.
9. Thompson D, Wallace J (2000) Annular modes in the extratropical circulation. Part I: Month-to-month variability. *J Clim* 13:1000–1016.
10. Holland M, Bitz C, Tremblay B (2006) Future abrupt reductions in the Summer Arctic sea ice. *Geophys Res Lett*, 10.1029/2006GL028024.
11. Serreze M, Holland M, Stroeve J (2007) Perspectives on the Arctic's shrinking sea-ice cover. *Science* 315:1533–1536.
12. Wang M, Overland J (2009) A sea ice free summer Arctic within 30 years? *Geophys Res Lett*, 10.1029/2009GL037820.
13. Alexander M, et al. (2004) The atmospheric response to realistic Arctic sea ice anomalies in an AGCM during winter. *J Clim* 17:890–905.
14. Magnusdottir G, Deser C, Saravanan R (2004) The effects of North Atlantic SST and sea ice anomalies on the winter circulation in CCM3. Part I: Main features and storm track characteristics of the response. *J Clim* 17:857–876.
15. Deser C, Magnusdottir G, Saravanan R, Phillips A (2004) The effects of North Atlantic SST and sea ice anomalies on the winter circulation in CCM3. Part II: Direct and indirect components of the response. *J Clim* 17:877–889.
16. Singarayer J, Bamber J, Valdes P (2006) Twenty-first-century climate impacts from a declining Arctic sea ice cover. *J Clim* 19:1109–1125.
17. DeWeaver E, Bitz C, Tremblay L (2008) *Arctic Sea Ice Decline: Observations, Projections, Mechanisms, and Implications* (American Geophysical Union, Washington, DC).
18. Kumar A, et al. (2010) Contribution of sea ice loss to Arctic amplification. *Geophys Res Lett*, 10.1029/2010GL045022.
19. Deser C, Tomas R, Alexander M, Lawrence D (2010) The seasonal atmospheric response to projected Arctic sea ice loss in the late 21st century. *J Clim* 23:333–351.
20. Honda M, Inoue J, Yamane S (2009) Influence of low Arctic sea-ice minima on anomalously cold Eurasian winters. *Geophys Res Lett*, 10.1029/2008GL037079.
21. Ghatak D, Frei A, Gong G, Stroeve J, Robinson D (2010) On the emergence of an Arctic amplification signal in terrestrial Arctic snow extent. *J Geophys Res*, 10.1029/2010JD014007.
22. Comiso J, Parkinson C, Gersten R, Stock L (2008) Accelerated decline in the Arctic sea ice cover. *Geophys Res Lett*, 10.1029/2007GL031972.
23. Stroeve J, Holland M, Meier W, Scambos T, Serreze M (2007) Arctic sea ice decline: Faster than forecast. *Geophys Res Lett*, 10.1029/2007GL029703.
24. Perovich D, Richter-Menge J, Jones K, Light B (2008) Sunlight, water, and ice: Extreme Arctic sea ice melt during the summer of 2007. *Geophys Res Lett*, 10.1029/2008GL034007.
25. Jackson J, Carmack E, McLaughlin F, Allen S, Ingram R (2010) Identification, characterization, and change of the near surface temperature maximum in the Canada Basin, 1993–2008. *J Geophys Res*, 10.1029/2009JC005265.
26. Overland J, Wang M (2010) Large-scale atmospheric circulation changes associated with the recent loss of Arctic sea ice. *Tellus A Dyn Meteorol Oceanol* 62A:1–9.
27. Screen J, Simmonds I (2010) The central role of diminishing sea ice in recent Arctic temperature amplification. *Nature* 464:1334–1337.
28. Kurita N (2011) Origin of Arctic water vapor during the ice-growth season. *Geophys Res Lett*, 10.1029/2010GL046064.
29. Collins W, et al. (2006) The formulation and atmospheric simulation of the Community Atmosphere Model Version 3 (CAM3). *J Clim* 19:2144–2161.
30. Hurrell J, Hack J, Shea D, Caron J, Rosinski J (2008) A new sea surface temperature and sea ice boundary dataset for the Community Atmosphere Model. *J Clim* 21:5145–5153.
31. Arzel O, Fichefet T, Goosse H (2006) Sea ice evolution over the 20th and 21st centuries as simulated by current AOGCMs. *Ocean Model* 12:401–415.
32. Holland M, Serreze M, Stroeve J (2010) The sea ice mass budget of the Arctic and its future change as simulated by coupled climate models. *Clim Dynam* 32:185–200.
33. Fetterer F, Knowles K, Meier W, Savoie M (2002) *Sea Ice Index* (National Snow and Ice Data Center, Boulder, CO) (updated 2009).
34. Kanamitsu M, et al. (2002) NCEP/DOE AMIP-II Reanalysis (R-2). *Bull Amer Meteorol Soc* 83:1631–1643.
35. Saha S, et al. (2010) The NCEP climate forecast system reanalysis. *Bull Amer Meteorol Soc* 91:1015–1057.
36. Thompson D, Wallace J (2001) Regional climate impacts of the Northern Hemisphere annular mode. *Science* 293:85–89.